Atomistic simulations of the pressure-induced phase transitions in BaF_2 crystals

2001 J. Phys.: Condens. Matter 13 11741

(http://iopscience.iop.org/0953-8984/13/50/334)

INSTITUTE OF PHYSICS PUBLISHING JOURNAL OF PHYSICS: CONDENSED MATTER

J. Phys.: Condens. Matter **13** (2001) 11741–11749 PII: S0953-8984(01)24145-9

Atomistic simulations of the pressure-induced phase transitions in BaF_2 crystals

A P Ayala

Departamento de Física, Universidade Federal do Ceará, Caixa Postal 6030, 60451-970, Fortaleza, Ceará, Brazil

E-mail: ayala@fisica.ufc.br

Received 20 April 2001, in final form 21 September 2001
Published 30 November 2001
Online at stacks.iop.org/JPhysCM/13/11741

Abstract

The pressure-induced sequence of phase transitions of the BaF_2 fluorite was studied within the shell-model approach. This fluorite crystal presents two pressure-induced phase transitions at approximately 3 and 15 GPa. The interatomic potentials were calculated by using relevant physical properties measured at ambient conditions. These potentials were used to minimize the lattice enthalpy at high hydrostatic pressures. By comparing the enthalpies and lattice parameters of the three possible structures, it was possible to describe the complete phase transition sequence of the material. The model reliability is confirmed by a comparison with experimental results reported at ambient conditions, which are in good agreement with the model predictions.

1. Introduction

Under ambient conditions, divalent metal halides AF_2 (A = Pb, Ca, Sr, Ba, etc) generally crystallize in the cubic fluorite structure. Crystals with this structure have been largely studied due to their applications as scintillation detectors and superionic conductors. In particular, barium fluoride (BaF_2) is a high-density luminescent material which is largely used for γ-ray and elementary particle detection [1].

The influence of the hydrostatic pressure on the properties of fluorite compounds has been studied by different techniques. In general, the pressure dependence of the elastic coefficients, dielectric constant, lattice parameters and Raman spectra suggests the existence of, at least, one structural transformation into an orthorhombic phase at high pressures. This behaviour was confirmed in BaF_2, CaF_2, PbF_2 and SrF_2 crystals [2–6].

Recently, different simulation techniques were used to study the pressure-induced transformations in AF_2 fluorites. In this way, quantum-mechanical *ab initio* calculations and first-principles pairwise simulations in CaF_2 [7] reproduced the phase transition observed in this material at ∼8 GPa. In PbF_2, *ab initio* calculations were successful for describing the

pressure-induced transitions, which include a hexagonal phase above 15 GPa [8]. The equation of state of the cubic and orthorhombic polymorphs of SrF_2 have been studied by using electron gas interionic potentials [9]. Despite the large number of simulations carried out on BaF_2 at ambient conditions [10] or high temperatures [11], no previous work has been published dealing with the stability of BaF_2 crystalline structures as a function of hydrostatic pressure.

In this paper, the phase transitions induced by hydrostatic pressure in BaF_2 are studied in the framework of the shell-model approach. A reliable set of interatomic parameters was derived which yields a good description of the crystal over a wide range of hydrostatic pressures. By using this method, the hydrostatic pressure is directly included in the lattice enthalpy allowing a direct comparison between calculated and experimental data.

2. Crystal structures

BaF_2, at ambient conditions, presents the cubic fluorite structure (β-BaF_2), which consists of three interpenetrating monatomic fcc sublattices, one of them occupied by barium and two by fluorine ions, and belongs to the cubic $Fm\bar{3}m$ space group with four molecules per unit cell. In this structure, [111] planes of cations are sandwiched between pairs of [111] planes of one or the other anion sublattices originating an eightfold cation coordination. Under hydrostatic pressure, two phase transitions are induced in BaF_2 crystals. At about 3 GPa, the fluorite phase transforms into the α-phase, which has an orthorhombic cotunnite-type structure ($PbCl_2$, $Z = 4$) [6]. In the cotunnite structure, one barium and two non-equivalent fluorine ions are at special 4c positions of the $Pnam$ space group. The nature of the β–α transformation can be depicted by considering that the cations dislocate in the [111] directions, half of them to the adjacent upper plane and the others to the adjacent lower plane. The cation coordination number in α-BaF_2 increases to 9, but not all nine anions are equivalent.

Under ambient conditions or at high pressures, over 400 compounds adopt the orthorhombic cotunnite structure [12]. Although the cotunnite structure presents the highest coordination observed in AX_2 compounds at ambient conditions, several compounds transform into a highly coordinated phase at high pressures. In the case of ACl_2 (A = Pb, Ba, and Sn) and $BaBr_2$, the new phase has a monoclinic structure ($P112_1/a$, $Z = 8$), where the metal ion has a tenfold coordination number [13, 14]. On the other hand, lead [8, 15] and barium [6] fluorides follow a different path transforming into a hexagonal Ni_2In-type structure ($P6_3/mmc$, $Z = 2$). The high-pressure phase of BaF_2, labelled as γ, was observed by x-ray diffraction above 15 GPa [6]. Both orthorhombic and hexagonal phases are built up of layers of trigonal prisms. The layers are directed along the orthorhombic $\boldsymbol{a}_o$-axis and the prisms share an edge parallel to the $\boldsymbol{c}_o$-axis. The phase transformation is characterized by the arrangement of the prisms, which form a corrugated layer in the orthorhombic phase and are aligned with the $\boldsymbol{a}_o$-axis in the hexagonal phase. The latest structure can also be presented in an orthorhombic description, using the space group $Pnam$ and the lattice parameters $\boldsymbol{a}_o = \boldsymbol{c}_h$, $\boldsymbol{b}_o = \sqrt{3}\boldsymbol{a}_h$ and $\boldsymbol{c}_o = \boldsymbol{a}_h$. In the orthorhombic basis, the atomic positions of the Ba and the two non-equivalent F are $(\frac{1}{4}, \frac{1}{12}, \frac{1}{4})$, $(\frac{1}{4}, \frac{5}{12}, \frac{1}{4})$ and $(0, \frac{1}{4}, \frac{3}{4})$, respectively. As a consequence of the layer alignment, the barium coordination number increases to 11 in the α-phase, the highest found in ionic materials.

3. Method

The ionic interactions in BaF_2 are simulated using the shell-model method, developed by Dick and Overhauser [16], which have been widely used to simulate halide fluorites with excellent

results [10, 17, 18]. In this model, each ion consists of a charged core and a charged shell, coupled by one harmonic spring. It is well established that the interactions between ion shells in ionic materials such as BaF_2 can be well represented by a two-body interatomic potential consisting of a long-range coulombic part and a short-range part, which is represented by the Buckingham expression

$$V_{ij} = z_i z_j e^2/r + A_{ij} \exp(-r/\rho_{ij}) - C_{ij}/r^6 \tag{1}$$

where i and j label the ionic species, and z_i is the charge of species i in units of the protonic charge. The three terms in equation (1) represent, respectively, the Coulomb interaction, the repulsive interaction due to overlap of the electron clouds and the van der Waals interaction. The dipolar polarizability of the ions has also been included through the use of the shell model [16]. The ions are assumed to have massless shells, charged with a charge Y_i, harmonically coupled to cores with a force constant K_i, i.e.,

$$E_{\text{core-shell}} = \tfrac{1}{2} K_i r^2. \tag{2}$$

All interatomic potentials act over the shell, which leaves the core coulombically screened, yielding an environment-dependent ion polarizability ($\alpha_i = Y_i^2/K_i$). All calculations have been performed using the program GULP [19] which optimizes the structure with respect to the asymmetric unit fractional coordinates and cell strains, using analytical symmetry-adapted first and second derivatives within a Newton–Raphson procedure starting from the exact Hessian matrix. Full details of the methodologies used by the program can be found elsewhere [19, 20].

In this paper, the parameters of the short-range interatomic potentials, A_{ij}, ρ_{ij} and C_{ij}, as well as the shell parameters, Y_i and K_i, were determined from the best fit to reproduce adequately some physical properties of the BaF_2 cubic structure. These properties were dielectric constants (static and high frequency), elastic constants and zone-centre phonon frequencies, which are acoustic (ω_{AC}), Raman-active (ω_R) and transverse infrared-active (ω_{TO}) phonons [21]. Even though the calculations carried out in this paper do not include the temperature explicitly, the potentials implicitly include thermal effects because they were fitted to experimental data obtained at room temperature. This statement will be confirmed later due to the remarkable agreement between the simulated and observed phase transition sequence. In a cubic $m\bar{3}m$ system, the dielectric and elastic tensors have one and three independent components, respectively. Furthermore, the zone-centre phonon energies are triply degenerate. In consequence, by including the constraint that the lattice energy derivative must be zero, fifteen observables were used to fit the nine parameters of the potential model. In this way a sufficient number of physical conditions were used in order to obtain a reliable parametrization. Table 1 shows the experimental results together the calculated values obtained by using the refined interatomic potentials. The overall good agreement between the two sets of parameters indicates the reliability of the interatomic potential derived for BaF_2. The adjusted coefficients of the interatomic potentials are shown in table 2; these are in good agreement with the previously reported data [10, 22].

4. Results and discussion

In order to generate thermodynamic data at finite pressures, the previously determined BaF_2 interatomic potentials were used and the lattice enthalpy was optimized with respect to all internal variables for each pressure. Since in the β-phase all atoms are at special sites of the cubic phase, only the lattice parameter is free to relax in order to minimize the lattice enthalpy. On the other hand, in the orthorhombic phase, there are one barium and two non-equivalent fluorine ions at special 4c positions (x, y, $\frac{1}{4}$), i.e. two degrees of freedom per atom;

Table 1. Experimental and calculated bulk properties of BaF_2 crystal [21].

	Experimental	Calculated
r_0 (Å)	6.2000	6.2421
ε_0	7.03	7.01
ε_∞	2.15	2.26
C_{11} (10^{12} dyn cm^{-2})	8.91	8.75
C_{12} (10^{12} dyn cm^{-2})	4.02	3.62
C_{44} (10^{12} dyn cm^{-2})	2.53	2.55
ω_{AC} (cm^{-1})	0	0.34
ω_{TO} (cm^{-1})	189	189
ω_R (cm^{-1})	241	241

Table 2. Short-range potentials and shell-model parameters for BaF_2 crystal.

	Shell–shell interactions		
	A (eV)	ρ (Å)	C (eV Å^6)
Ba–F	1779.3	0.3235	
F–F	237.0	0.3674	90.29
	Core–shell interactions		
	k(eV Å^2)	$Y(e)$	
Ba	557.9	11.49	
F	271.4	−2.99	

furthermore, on including the orthorhombic cell lattice dimensions, nine parameters must be relaxed. Finally, the hexagonal phase was simulated by using its orthorhombic description and fixing the ions at the corresponding positions. Thus, in the hexagonal phase only the lattice parameters were free to relax. The lattice enthalpies of the cubic and orthorhombic phases at ambient conditions are −95.974 and −95.530 eV per unit cell, respectively. Furthermore, they exhibit linear pressure behaviours with similar slopes. Since these phases have very close enthalpy values, the best way of investigating their pressure dependence is by plotting the difference of the lattice enthalpies. Thus, in figure 1(a), the difference between the lattice enthalpies of the β- and α-phases is plotted as a function of the hydrostatic pressure. It is observed that the cubic phase has lower lattice energy than the orthorhombic one under 3.3 GPa. Above this pressure, the orthorhombic phase becomes more stable. Note the remarkable agreement with the experimental ∼3.0 GPa value [4]. It is interesting to notice that the enthalpy difference between the two phases is less than 1% of the lattice enthalpy. Thus, small errors in the potentials can lead to strong deviations in the critical pressure. However, the good agreement between the experimental and calculated transition pressures attests to the reliability of the results presented in this paper.

As was already pointed out, above 15 GPa, α-BaF_2 undergoes another phase transformation into the hexagonal γ-phase. By using an orthorhombic cell to describe the γ-phase, a direct comparison of the lattice enthalpies with the orthorhombic α-phase is possible, since the number of molecules per unit cell is preserved. In view of this, in figure 1(b) the difference between the orthorhombic and hexagonal lattice enthalpies is plotted; this shows that below 15 GPa the most stable phase is the orthorhombic one. Above this pressure the two phases have the same lattice enthalpy, suggesting a continuous transformation between α- and γ-structures.

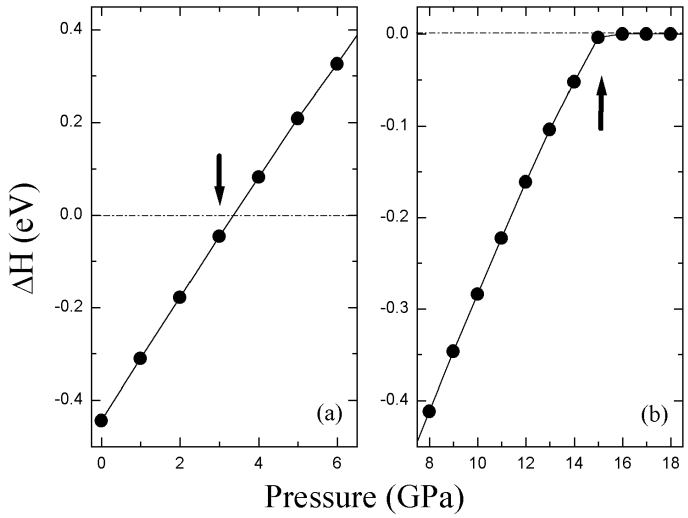

Figure 1. Difference of the enthalpies per unit cell for the (a) cubic and orthorhombic lattices and (b) orthorhombic and hexagonal lattices, as functions of the hydrostatic pressure. Arrows indicate the experimental critical pressures.

The lattice parameters obtained by relaxing all structures under hydrostatic pressure are plotted in figure 2, where the orthorhombic lattice parameter $\boldsymbol{b}_o$ is shown divided by $\sqrt{3}$ in order to accomplish a better comparison with the corresponding hexagonal parameter ($\boldsymbol{a}_h$). In the same figure, the experimental data measured by Leger *et al* [6] are included. The pressure of the transformation between the β- and α-phases was determined by the crossover of the lattice enthalpies ($\Delta H = 0$) present in figure 1(a), since no evidence of this transition was observed in the lattice parameter behaviour. Both β- and α-phase lattice parameters are well reproduced in the present calculations. In particular, the volume change found in the transformation from fluorite to cotunnite structure is -10.1%, which is the largest value observed in this kind of phase transition [12, 23]. Furthermore, Leger *et al* [6] noticed that, at atmospheric pressure after decompression, a mixture of orthorhombic and cubic phases is observed. Although the model used here does not reproduce any metastability, the lattice parameters calculated in the orthorhombic polymorph below the critical pressure agree very well with the experimental parameters of the metastable α-phase (also shown in figure 2).

The second crystallographic transformation becomes clear in figure 2. Since the hexagonal phase is described in the orthorhombic basis, the $\boldsymbol{b}_o/\sqrt{3}$ parameter becomes equal to $\boldsymbol{c}_o$ when the phase transformation is completed. In this way, it is possible to observe the continuous transformation between α- and γ-BaF_2 structures, which is completed above 17 GPa. This result confirms the observations by Leger *et al* [6]. These authors pointed out that the phase transformation is completed only above the pressure predicted in the present work. It is important to notice that the hexagonal phase is not imposed in the simulation; the system naturally relaxes to this phase at high hydrostatic pressures. In general, the results of Leger *et al* [6] are well reproduced by the simulation, but in the hexagonal phase some discrepancies are observed in the values of the $\boldsymbol{c}_h$-axis parameter. This result should be indicative of the model limitations, but it is important to notice that the $\boldsymbol{a}_h$-axis parameter behaviour is reproduced. In consequence, the discrepancies should also be of experimental origin, since at high pressure the transmitting medium (silicone grease) should solidify, producing a quasi-hydrostatic pressure.

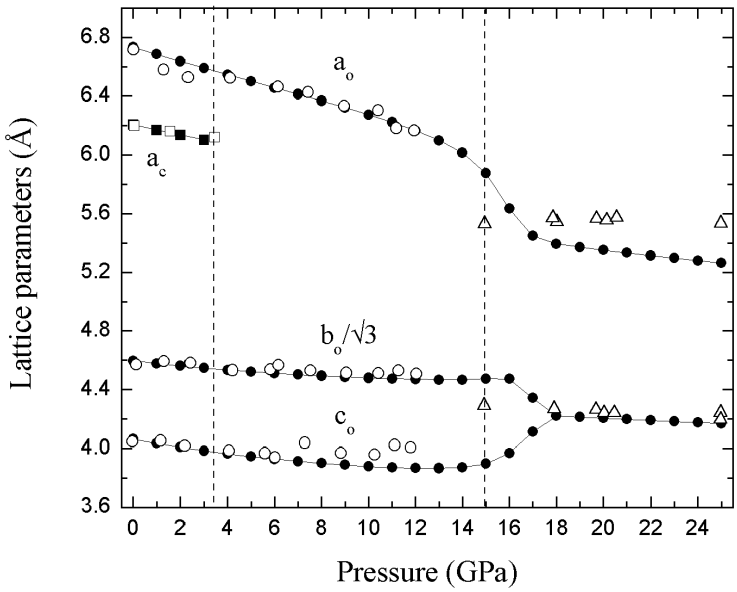

Figure 2. Lattice parameters as functions of the hydrostatic pressure. Solid symbols indicate the values calculated in this work. Open symbols indicate the experimental results obtained by Leger *et al* [6].

Despite small discrepancies with the experimental results, shell-model simulations reproduce not only the phase transition sequence but also the critical pressure values.

The continuous character of this phase transformation can also be observed in the behaviour of the internal coordinates shown in figure 3. As was pointed out, the orthorhombic space group is a subgroup of the hexagonal one. In view of this, the hexagonal structure should be described in an orthorhombic basis with atoms placed at some special positions (indicated by dashed lines in figure 3). Thus, on allowing the orthorhombic structure to relax to equilibrium values after increasing the pressure, the internal coordinates converge to values corresponding to those of the hexagonal structure and then remain unchanged, although the simulation does not impose them being fixed above 17 GPa. These results support also the assertion that the γ-phase is the most stable structure above 17 GPa, since the structural conditions that determine this phase are fulfilled, i.e. $\boldsymbol{b}_o/\sqrt{3} = \boldsymbol{c}_o$, and the atoms are placed at the positions indicated by dashed lines in figure 3.

The reliability of the shell-model calculations presented here can also be checked by comparing some physical properties derived from the model with the corresponding experimental data. As an example, the values of the bulk modulus (B_0), which is a function of the elastic constants, obtained in the present work are 50 GPa (cubic), 70 GPa (orthorhombic) and 133 GPa (hexagonal), which are very close to those estimated by Leger *et al* [6] near the phase transitions (57, ∼82 and ∼125 GPa respectively).

The β–α transformation in the BaF_2 crystal was also observed by Samara [4, 5], who studied the pressure dependence of the sample capacitance. After normalizing Samara's data using the static dielectric constant calculated at atmospheric pressure, comparison between the shell-model results and Samara's data becomes possible. Thus, in figure 4(a), the calculated static dielectric constants are plotted as a function of the hydrostatic pressure. In the same plot, the normalized experimental values are included. The agreement between the experimental

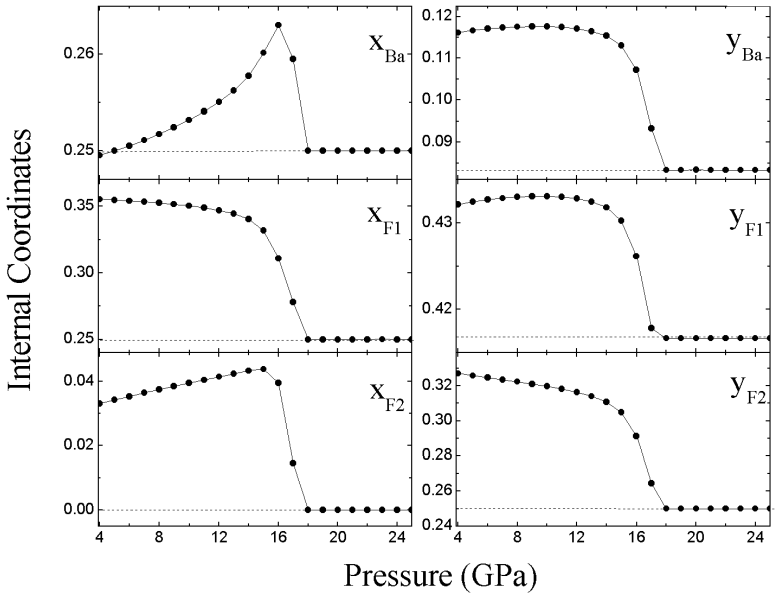

Figure 3. Internal coordinates for the orthorhombic phase as functions of the hydrostatic pressure. Dotted lines represent the corresponding atomic positions in the hexagonal phase.

and calculated data in the cubic phase is excellent, but experimental values in the orthorhombic phase are rather poor. It can be noticed that in the cited references the crystal was not oriented, leading to an average value of the static dielectric constant in the orthorhombic phase and underestimating the jump of the static dielectric constant. Concerning all results, it is important to remark that a new anomaly is observed in the static dielectric constant at the β–γ transformation. Due to the continuous character of this transition, no sharp jump is expected, as observed. On the other hand, for the hexagonal structure, where $\boldsymbol{c}_h = \boldsymbol{a}_o$, the ϵ_0-components in the $\boldsymbol{a}_h\boldsymbol{b}_h$-plane ($\boldsymbol{c}_o\boldsymbol{b}_o$-plane) are equal. To our knowledge, there are no reported measurements concerning the pressure dependence of the high-frequency dielectric constant of BaF_2, but this result can also be obtained from shell-model calculations. Thus, figure 4(b) presents the pressure dependence of all components of the high-frequency dielectric constant in each phase. This figure clearly shows that ε_∞ increases continuously in β, α and γ phases, with a large jump at the first phase transformation and a sigmoidal-like increase at the second one, compatible with the character of these transitions.

At this point, the α–γ transformation mechanism deserves to be discussed in more detail. As was previously pointed out, the highest-pressure phases are constituted by layers of trigonal prisms, which are corrugated and aligned in the orthorhombic and hexagonal phases, respectively. In figure 5(a), the $\boldsymbol{a}_o\boldsymbol{b}_o$-plane is shown, where the corrugated arrangement of trigonal prisms can be observed and the tilt angle among them is indicated. According to the proposed model, the prisms should align progressively due to the continuous character of the phase transformation. That this in fact occurs can be verified by observing figure 5(b), where the tilt angle is plotted as a function of the pressure. This angle goes continuously to zero when BaF_2 transforms between the α- and γ-polymorphs.

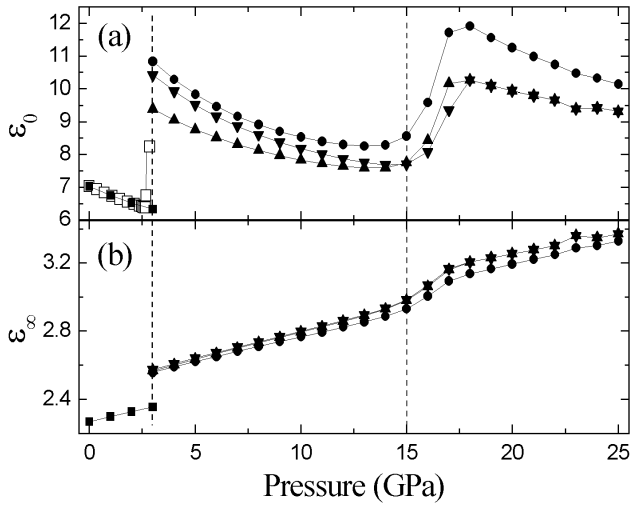

Figure 4. (a) Static and (b) high-frequency dielectric constants as functions of the hydrostatic pressure. Solid symbols represent the non-zero components of the static or high-frequency dielectric constant in the cubic (■, zz) and orthorhombic (●, xx; ▲, yy; ▼, zz) phases. Open symbols (□) show the experimental values obtained by Samara [4].

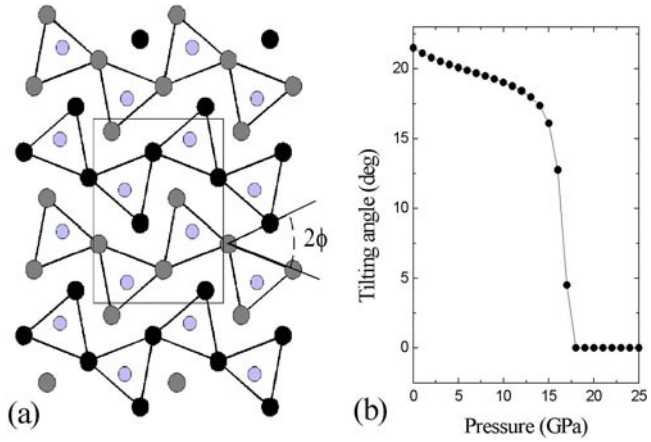

Figure 5. (a) Projection of the cotunnite structure on the xy-plane. Light grey, black and grey circles represent Ba, F at z and F at $z + \frac{1}{2}$. (b) The tilt angle of the trigonal prisms as a function of the hydrostatic pressure.

(This figure is in colour only in the electronic version)

5. Conclusions

The sequence of pressure-induced phase transition of BaF_2 was simulated by using an atomistic calculation based on the shell model. A set of reliable interionic potentials for BaF_2 was developed in the framework of the shell-model approach. This model is able to successfully reproduce the structural, elastic and dielectric properties of the fluorite structure of the material. The interatomic potentials estimated under ambient conditions were used to calculate the lattice enthalpy of the BaF_2 polymorph at finite hydrostatic pressures. From these calculations,

not only was the phase transition sequence reproduced, but also the critical pressure values are in excellent accord with experimental observations. The computed lattice dimensions and dielectric constant as functions of the pressure for the fluorite structure agree with the experimental results, and extend the information on the dielectric behaviour to a large pressure range. Detailed information about the atomic positions was obtained, which allows a good description of the orthorhombic–hexagonal phase transition mechanism. Since this method consumes less time than *ab initio* calculations and reproduces very well the observed physical properties, atomistic simulations seem to be an excellent technique for studying the effect of the hydrostatic pressure on ionic crystals.

Acknowledgments

I thank Professor Roberto Luiz Moreira and Professor Ilde Guedes for a critical reading of the manuscript and Julian Gale for the permission to use the GULP code. This work was partially supported by the Brazilian agencies CNPq and FUNCAP.

References

[1] Weber M J, Lecoq P, Ruchti R C, Woody C, Yen W M and Zhu R Y (ed) 1994 *Scintillator and Phosphor Materials (MRS Symp. Proc. No 348)* (Pittsburgh, PA: Materials Research Society)
[2] Smith H I and Chen J H 1966 *Bull. Am. Phys. Soc.* **11** 414
[3] Dandekar D P and Jamieson J C 1969 *Trans. Am. Crystallogr. Assoc.* **5** 19
[4] Samara G A 1970 *Phys. Rev.* B **2** 4194
[5] Samara G A 1976 *Phys. Rev.* B **13** 4529
[6] Leger J M, Haines J, Atouf A, Schulte O and Hull S 1995 *Phys. Rev.* B **52** 13 247
[7] Martín Pendás A, Recio J M, Flóres M, Luaña V and Bermejo M 1994 *Phys. Rev.* B **49** 5858
[8] Costales A, Blanco M A, Pandey R and Recio J M 2000 *Phys. Rev.* B **61** 11 359
[9] Francisco E, Blanco M A and Sanjurjo G 2001 *Phys. Rev.* B **63** 094107
[10] Vail J M, Emberly E, Lu T, Gu M and Pandey R 1998 *Phys. Rev.* B **57** 764
[11] Zhou L X, Hardy J R and Cao H Z 1996 *Solid State Commun.* **98** 341
[12] Hyde B G, O'Keeffe M, Lyttle W M and Brese N E 1992 *Acta Chem. Scand.* **46** 216
[13] Léger J M, Haines J and Atouf A 1995 *Phys. Rev.* B **51** 3902
[14] Léger J M, Haines J and Atouf A 1996 *J. Phys. Chem. Solids* **57** 7
[15] Lorenzana H E, Lipp M J, Evans W J, Radousky H B and van Schilfgaarde M 1997 *Phys. Rev.* B **56** 543
[16] Dick B G and Overhauser A W 1958 *Phys. Rev.* **112** 90
[17] Lindam P J D and Gillan M J 1993 *J. Phys.: Condens. Matter* **5** 1019
[18] Jiang H, Costales A, Blanco M A, Gu M, Pandey R and Gale J 2000 *Phys. Rev.* B **62** 803
[19] Gale J D 1997 *J. Chem. Soc. Faraday Trans.* **93** 629
[20] Gale J D 1996 *Phil. Mag.* B **73** 3
[21] Hayes W 1974 *Crystals with Fluorite Structure: Electronic, Vibrational and Defect Properties* (Oxford: Clarendon) and references therein
[22] Catlow C R A, Norgett M J and Ross A 1977 *J. Phys. C: Solid State Phys.* **10** 1627
[23] Morris E, Groy T and Leinenweber K 2001 *J. Phys. Chem. Solids* **62** 1117